Manifold connections and the transport of small bodies through mean motion resonances in the Solar System 227

PhD SST
Space Science and Technology

Alessia Francesca Guido [1] Christos Efthymiopoulos [2]

[1]University of Trento [2]University of Padova

1. Introduction

We discuss how the transport of small bodies through the orbit of Jupiter in the Solar System is governed by the heteroclinic intersections between the stable and unstable manifolds of the unstable periodic orbits corresponding to each one of the main mean motion resonances between the body's and Jupiter's orbits [1],[3].

These manifolds have been extensively discussed in literature in the case of the co-orbital resonance. (manifolds of the periodic orbits around the collinear Lagrangian points, [2]), but to a lesser extent for other important mean motion resonances.

Method

Here we show how a global visualization of these manifolds can be achieved through the computation of short time Fast Lyapunov Indicator maps [4] [5], allowing to depict their underlying intricate heteroclinic dynamics (Figure 1 to 3).
A precise computation of these manifolds is decribed in section 3.

2. Computation of Fast Lyapunov Indicator

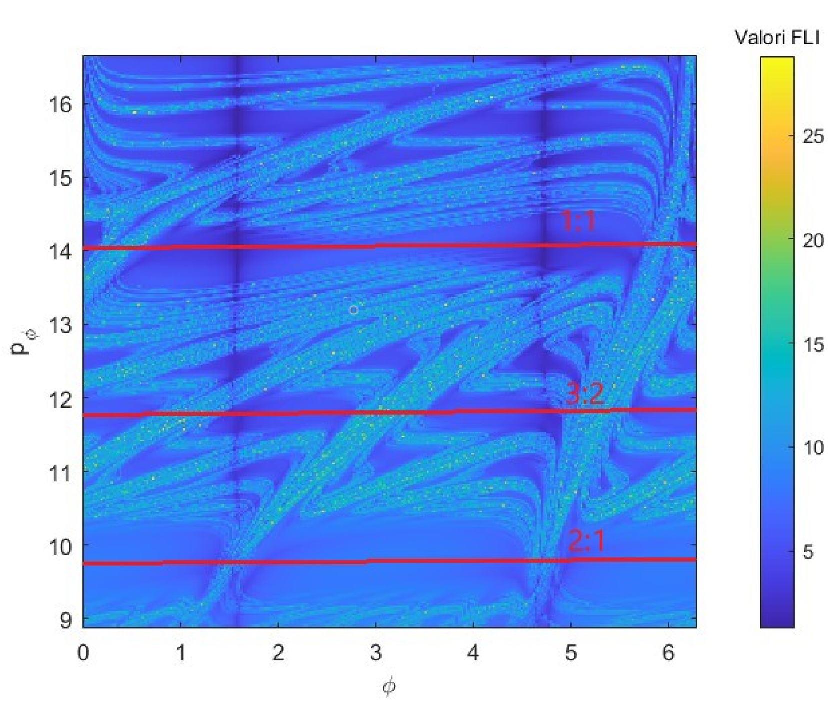

Figure 1. Color Representation of the chaos indicator FLI computed in an interval time $[0, 100]$ on a refined grid of polar initial conditions (φ,p_φ) regularly spaced on the phase-space; the value of $log(FLI)$ is represented using a color scale: on each point (φ,p_φ) of the grid we represent a pixel with a color corresponding to the value of $log(FLI)$: $log(FLI) = 0$ is reported in blu, $log(FLI) > 30$ is reported in yellow; the values intermediate between 0 and 30 are reported wit the color scale represented on the right of the panel.

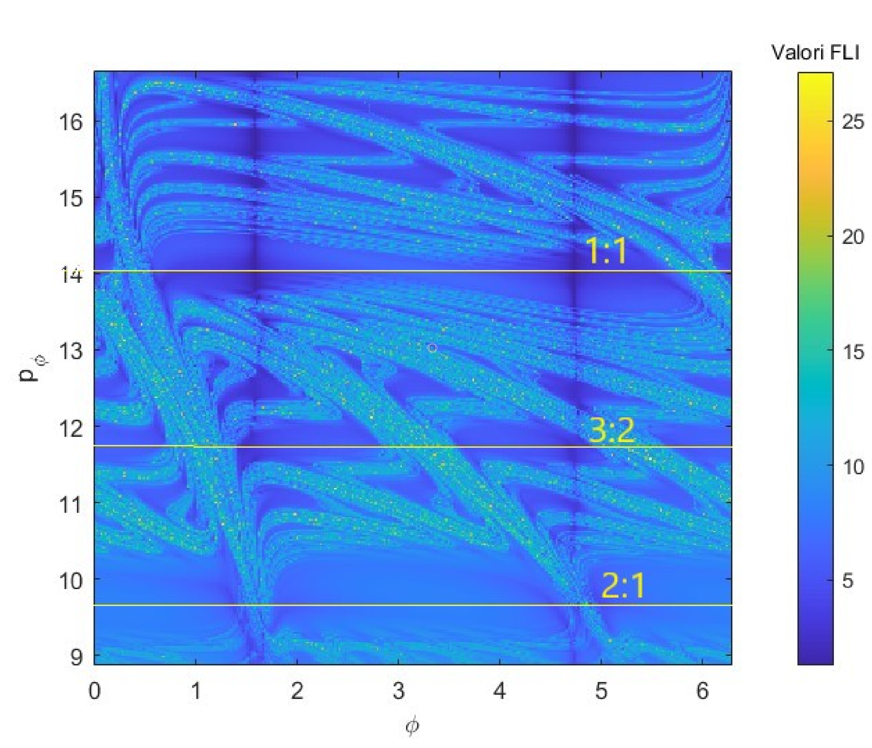

Figure 2. Color Representation of the chaos indicator FLI computed in an interval time $[0, -100]$.

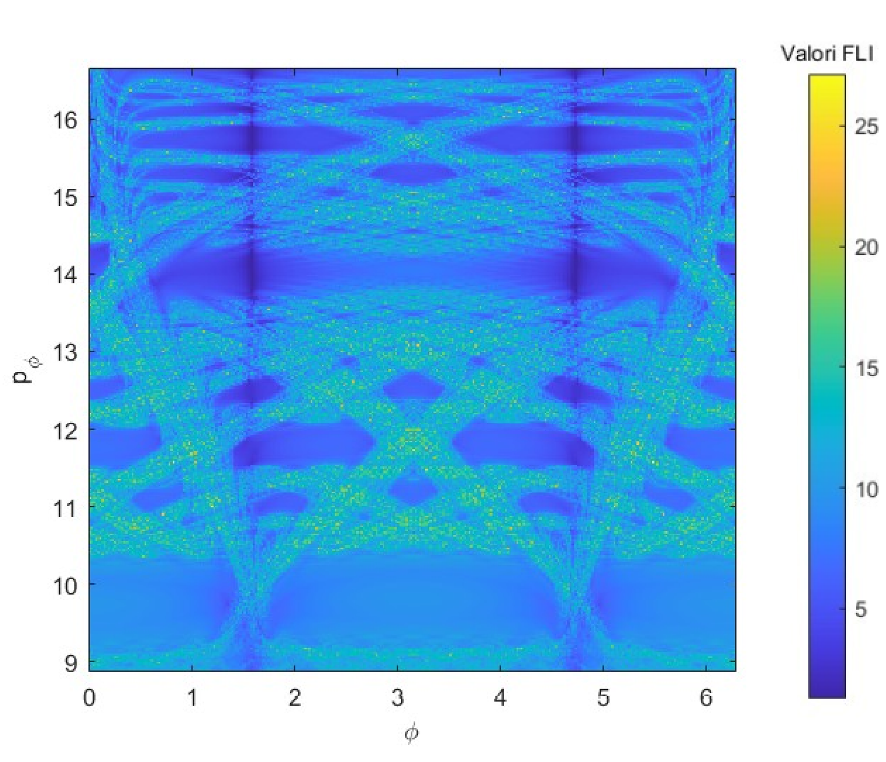

Figure 3. Overlap of the two plots (Figura 1.) and (Figura 2.)

The *FLI* (Fast Lyapunov Indicator) maps were obtained by integrating orbits forward and backward in time, while varying the initial values of φ and p_φ, in the planar circular restricted three body problem given by the hamiltonian:

$$H = \frac{1}{2}\left(p_r^2 + \frac{p_\varphi^2}{r^2}\right) - \omega p_\varphi - \frac{GM_S}{\sqrt{(r\cos\varphi - x_S)^2 + (r\sin\varphi)^2}} - \frac{GM_G}{\sqrt{(r\cos\varphi - x_G)^2 + (r\sin\varphi)^2}}$$

where (r, p_r),(φ, p_φ) are polar canonical coordinates.
By computing the *FLI* values for short times [6], one can visually observe structures representing the stable and unstable manifolds of various periodic orbits characterizing the phase space.

Figures 1 and 2 show the FLI maps depicting the dynamics around the 1:1 (co-orbital), 3:2 (Hildas), and 2:1 resonances, representing the stable and unstable manifolds associated with them, respectively.

We observe that near the resonances (identified by the yellow lines associated with specific values of p_φ), stability islands with periodic orbits at their center emerge.

Outside the stability islands (depicted by the blue areas), chaotic motion predominates with stable (Figure 1) and unstable (Figure 2) manifolds. Through FLI maps, a series of chaotic trajectories connecting different resonances identified in the map can be observed.

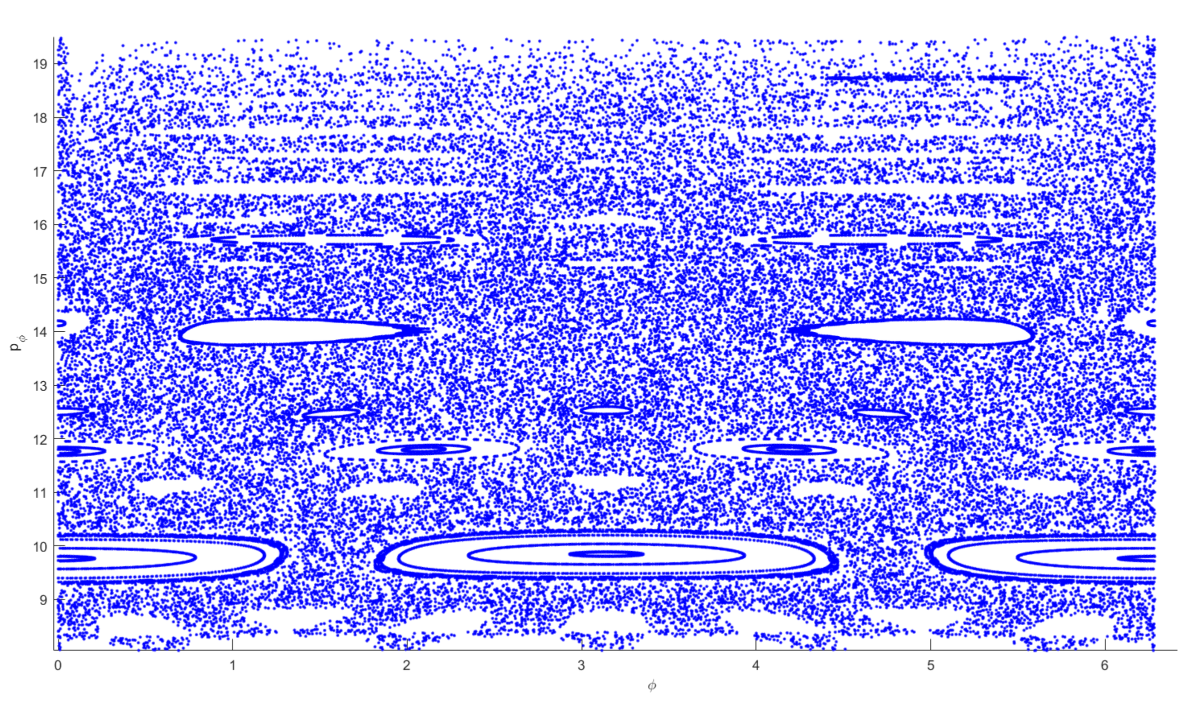

Figure 4. Section of Poincarè of the PCR3BP in the interval time $[0, 100]$ on a refined grid of polar initial condition: $\varphi \in [0, 2\pi]$, $p_\varphi \in [9, 16]$.The Poincaré section considered was the surface defined by $p_{r_0} = 0$.

A direct image of the corresponding phase portrait is obtained by the following steps:

- For the initial values, φ was fixed within the range $[0, 2\pi]$ and p_φ within the interval $[p_{\varphi_{min}}, p_{\varphi_{max}}]$. The initial value of p_{r_0} was set to zero.
- Given the Jacobi constant, the initial value r_0 was chosen such that $\dot{p_{r_0}} > 0$, r_0 represents the pericentric radius.
- A value for the Jacobi constant corresponding to $T = 2.96$ was set. ($2 \le T \le 3$ is the common range of the Tisserand parameter for Jupiter family comets and asteroids such as Trojans and Hildas). This was done to subsequently obtain a Poincaré section containing various types of orbits (Figure 4).

Conclusions

The main conclusion from Figure 1-6 is that the stable and unstable manifolds emanating from one mean-motion resonance extended to a large chaotic domain, thus they create heteroclinic intersections with the manifolds emanating from other mean motion resonances both at the interior or exterior to the orbit of Jupiter. The efficiency of transport of small bodies through the orbit of Jupiter, due to such intersection, is under investigation.

3. Computation of Stable-Unstable Manifolds with semi-analytical method

Using the Newton-Raphson method, coordinates representing an unstable periodic orbit, corresponding to 2:1 mean motion resonance, on the Poincaré section were identified and the monodromy matrix associated with this orbit was calculated [7].

Subsequently, along the directions determined by the stable/unstable eigenvectors of the monodromy matrix, we choosed N_p points and evaluate the Poincaré section with multiplicity, m equal to two. This process enabled obtaining an approximation, on the section, of the stable and unstable manifolds associated with this unstable periodic orbits.

Representation of Stable-Unstable Manifolds

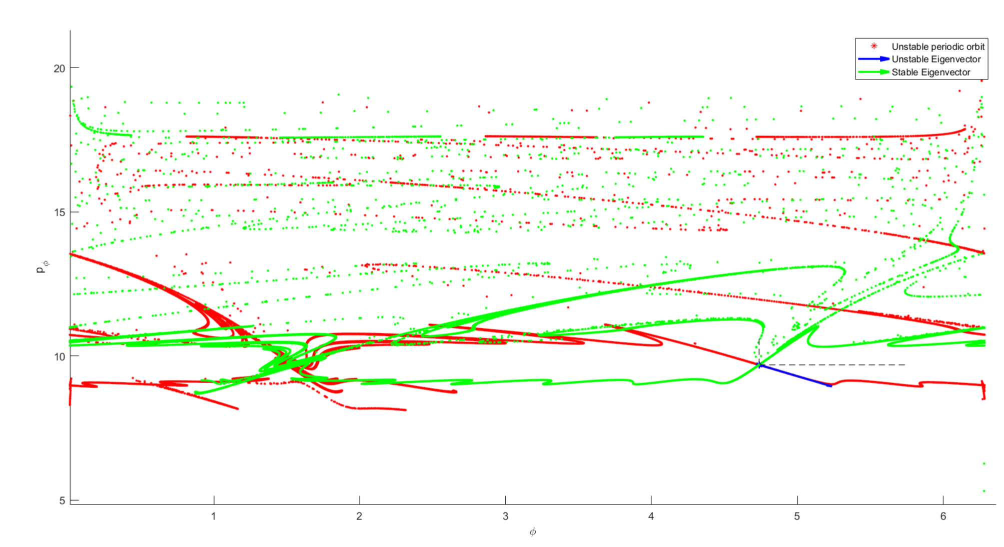

Figure 5. Representation of an approximation, using the monodromy matrix and poincaré section (both implemented), of unstable (red) and stable (green) manifolds associated to the unstable periodic orbit of coordinates ($\varphi = 1.545$,$p_\varphi = 9.689$).

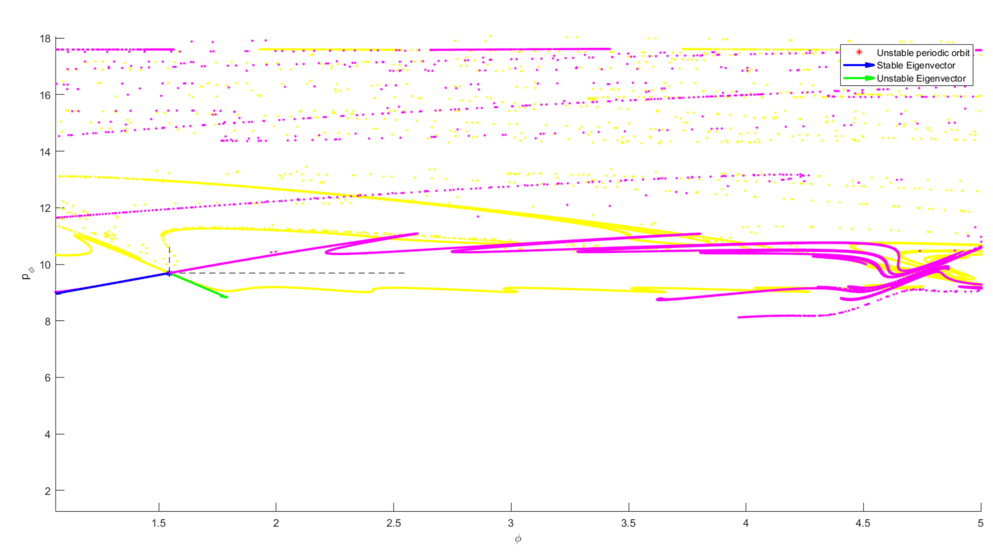

Figure 6. Representation of an approximation of unstable (yellow) and stable (purple) manifolds associated to the point ($\varphi = 4.738$,$p_\varphi = 9.689$)

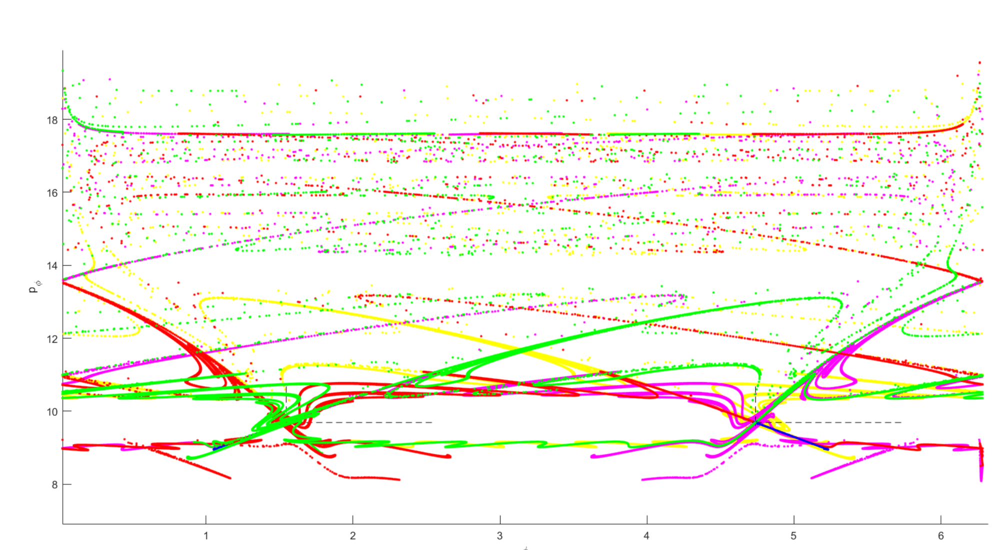

Figure 7. Overlap of Figure 5 and Figure 6

References

- [1] Koon W.S., Lo M.W., Marsden J.E., Ross S.D. (2000), *Heteroclinic connections between periodic orbits and resonance transitions in celestial mechanics* in: Chaos 10, 427–469.
- [2] Anderson R, Lo M., *A dynamical systems analysis of resonant flybys: ballistic case* in: J Astronaut Sci 2011;58. doi: 10.1007/BF03321164.
- [3] G. Gomez and J. M. Mondelo, (2001) *The Dynamics Around the Collinear Equilibrium Points of the RTBP* in:Physica, Vol. 157, No. 4, pp. 283–321 .
- [4] Nataša Todorović et al., (2020), *The arches of chaos in the Solar System* in: Science Advances Vol 6, Issue 48.
- [5] A. Celletti, Stability and Chaos in Celestial Mechanics, Springer-Verlag, Berlin; published in association with Praxis Publishing Ltd., Chichester, ISBN: 978-3-540-85145-5 (2010)
- [6] Guzzo, M., Lega, E. (2023), *Theory and applications of fast Lyapunov indicators to model problems of celestial mechanics* in: Celest Mech Dyn Astron 135, 37.
- [7] Topputo P (2015), *Fast Numerical Approximation of Invariant Manifolds in the Circular Restricted Three-Body Problem* in Commun. Nonlinear Sci. Num. Simulat., 32, pp. 89-98.

alessia.guido@unit.it

christos.efthymiopoulos@math.unipd.it